Characterization of Secondary Electron Emission Yield from Velvet-Type Materials

IEPC-2017-195

Presented at the 35th International Electric Propulsion Conference
Georgia Institute of Technology • Atlanta, Georgia • USA
October 8 – 12, 2017

Angelica Ottaviano,[1] Chenggang Jin, [2] Yevgeny Raitses[3]

Princeton Plasma Physics Laboratory, Princeton, NJ 08543, USA

and

Sankha Banerjee[4]
California State University, Fresno, CA 93740, USA

Abstract: Micro- and nano-engineered materials are predicted to have a small secondary electron emission (SEE) yield because their micro cavities should trap emitted electrons. These materials can be useful for various plasma applications including, but not limited to Hall thrusters [1]. It was previously demonstrated that the use of, for example, carbon velvet as the channel wall material for a Hall thruster can lead to dramatic improvements of insulating properties of magnetized thruster plasma allowing to reach significant dc electric field of ~ 1kV/cm. We report results of measurements of SEE yield from samples of carbon velvet with different packing densities and fiber lengths using an experimental setup for SEE measurements at PPPL [2]. A new simplified diagnostic technique is also proposed for qualitative measurements of SEE yield. Both methods of measurements of SEE properties demonstrated a significantly smaller SEE yield from these engineered materials as compared to graphite material and boron nitride. The results also demonstrate the existence of an optimal velvet configuration and are in agreement with a recent model of SEE yield from velvet [3].

Nomenclature

SEE = Secondary electron emission
PE = Primary electron
SE = Secondary electron
SEM = Scanning Electron Microscope

I. Introduction

SECONDARY electron emission (SEE) is known to affect the performance Hall thrusters [1-10]. SEE from the thruster channel walls can contribute to the enhancement of the electron cross-field current increasing and thereby, reducing the thruster efficiency [11-12].

A method for the reduction of SEE is to use surface architectured materials which reduce the flux of secondary electrons (SEs) from the wall [1-3]. By introducing micro and nano cavities on the surface of these materials such as grooves [13], pores [14-15], fuzz [16] or fibers [17-18], generated SEs become trapped and the net SEE yield of such a surface is reduced [2]. This work focuses on carbon velvet which has been used in Hall thruster applications

[1] Diagnostic Specialist, Physics Research and Development, Tri Alpha Energy Inc., angelica.ottaviano@gmail.com
[2] Post-doctoral Researcher, College of Physics, Soochow University, cjin@suda.edu.cn
[3] Principle Research Physicist, Department of Plasma Science and Technology, yraitses@pppl.gov
[4] Professor of Engineering, Mechanical Engineering, sankhab@csufresno.edu

for segmented electrodes as well as on channel walls [1]. The material consists of high aspect ratio carbon fibers bound to a graphite substrate. The fiber lengths range from 0.5mm to 3.0mm and their radii are ~3.5um. Recent theoretical and experimental studies have shown that the reduction in SEE yield for such velvets compared with a smooth graphite surface is of ~65% [19].

An overview of SEE measurements made for five different velvet samples is presented by using a similar experimental setup as explained in references [19] and [20], and they are compared to qualitative estimates of SEE yield obtained by a new simplified approach using a Scanning Electron Microscope (SEM) and image pixel intensity analysis. Since the SEE yield of carbon velvet depends on its surface features (fiber length, density and orientation [3]), SEM imaging has also been used to evaluate the fiber densities of the samples under consideration. The technique is particularly useful in the case where velvet's surface features are non-uniform and different from the manufacturing indications, as shown in Figure 1. For example, the specified fiber packing density is the ratio of fiber tips to total velvet area when fibers are aligned perpendicularly to the graphite base. If the fibers are not aligned the real fiber density is larger because it will also include side surface areas of the fibers. The samples analyzed in this work have indicated by manufacturing packing densities of 0.8-4.0%, but SEM has revealed that their true fiber densities are 59-90% larger.

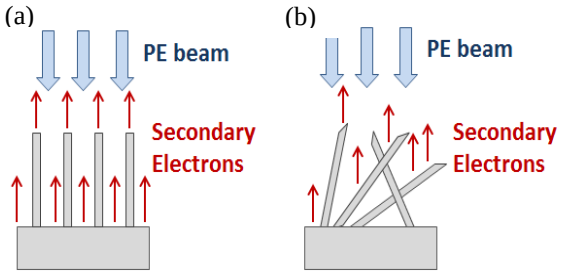

Figure 1. *Diagram of carbon velvet fibers aligned with incoming PE beam (a) and realistic carbon velvet fibers not aligned with PE beam (b).*

A summary of important results of SEE yield for high aspect ratio carbon velvets using both direct laboratory setups [19] and SEM techniques with incoming primary electron (PE) energies of 30-1000eV are reported.

II. Setup and Procedure

Velvets of varying fiber length and manufacturing density were analyzed for their surface and SEE properties using SEM at Princeton University's Imaging and Analysis Center, and by using a laboratory setup of an electron gun with a Faraday cup collection system at the Princeton Plasma Physics Laboratory. These are the same samples described in reference [19]. Each velvet surface was imaged with an Environmental SEM at 15keV for optimal resolution at a large depth of field [21] with low magnification producing image areas of ~1mmX 1mm. An example of a velvet SEM image is shown in Figure 2. These are processed as in reference [19] to calculate the actual fiber density as a percentage of fiber occupying a surface to total sample region.

To qualitatively evaluate the SEE yields of the imaged surfaces, a conversion factor from pixel intensity to SEE yield was determined. SEM functions on the principle of SEE, where the image pixel intensity (brightness) is directly proportional to the detector's signal strength, and is in turn directly proportional to the amount of SEs collected [21]. Images of smooth graphite were recorded alongside the velvet samples. Then the mean average pixel intensity was found of the smooth graphite images and set to be equal to SEE yield of smooth graphite (0.85 at 500eV PE beam energy and 0.75 at 1.0keV PE beam energy, [19]). Black pixels should indicate an SEE yield of 0. The conversion

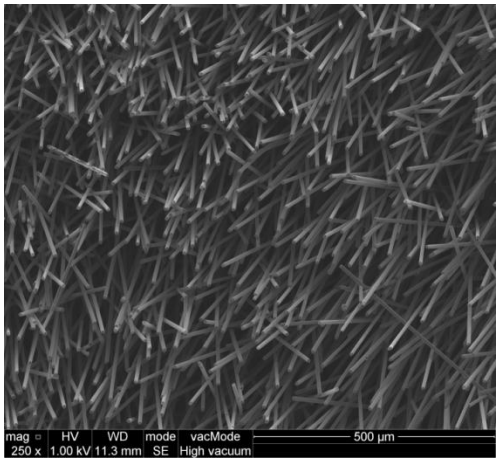

Figure 2. SEM image of a carbon velvet surface. *This micrograph was produced using a PE beam energy of 500eV and shows a sample surface with an actual fiber density of 78%, a fiber length of 1.5mm and a net SEY of 0.48.*

factor was therefore extrapolated to find the average SEE yield of velvet image based on its average pixel intensity. Each velvet region imaged by SEM was then analyzed for its real fiber density and also for its qualitative SEE yield estimates. The details of this technique will be reported on a separate journal paper.

III. Experimental Results

SEE yield measurements obtained using SEM analysis and laboratory setups reveal that for PE beam energies of 50-1000eV, carbon velvet with 1.5mm length fibers reduces SEE yield of smooth graphite by 29-65%. This result generally agrees with theoretical calculations [3] and with experimental findings [19] where the net SEE yield of a velvet surface is decreased compared to a smooth surface due to inter-fiber SE trapping. Theoretical models however predict that the total SEE yield reduction may be as high as 90% [3], but these models apply to velvets which have a true fiber density that matches their indicated manufacturing density which is when the fibers are as in Figure 1 (a).

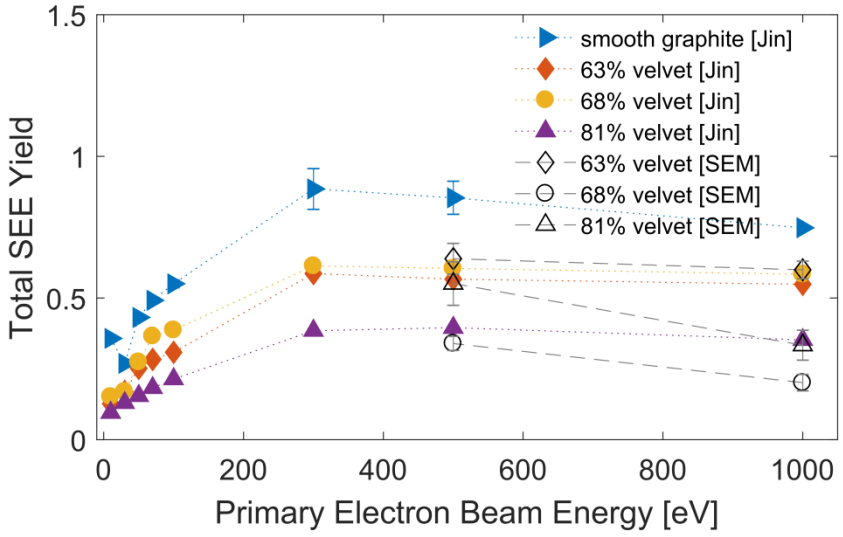

Figure 3. Total velvet SEE yield with varying primary electron beam energies. *The samples shown in this plot each have a fiber length of 1.5mm and varying fiber densities. SEE yield of 63% velvet (diamond marker), 68% velvet (circular marker) and 81% velvet (triangular marker) are measured with a direct setup [19] from 30-1000eV and with SEM at 500eV and 1000eV.*

The measurements shown in Figure 3 also indicate an optimized velvet configuration. In the direct measurements, the lowest SEE yield for velvet of fiber length 1.5mm is found for a 81% fiber density velvet (0.39 at 500eV), whereas SEM shows that this occurs for velvet of 68% fiber density (0.37 at 500eV). The discrepancies are due to the localization of the SEM method with respect to laboratory measurements. In an SEM analysis, the entire surface of the velvet can be surveyed and imaged, whereas with the direct electron gun method, the PE beam is roughly directed at a 1mmX1mm area, and it is difficult to measure the entire surface evenly.

Another interesting result is found by analyzing individual micrographs across the surface of one sample only. It appears that the net SEE yield across an imaged surface has a weakly linearly related to the amount of fiber surface exposed to the primary electron beam, or its actual fiber density. Figures 3 (a) and (b) plot the SEE yield and actual fiber densities per SEM micrograph of a velvet sample of 0.5mm fiber length and 85% real fiber density. Results are shown for incoming primary electron beam energies of 1.0keV Fig 3 (a) and 500eV Fig 3 (b).

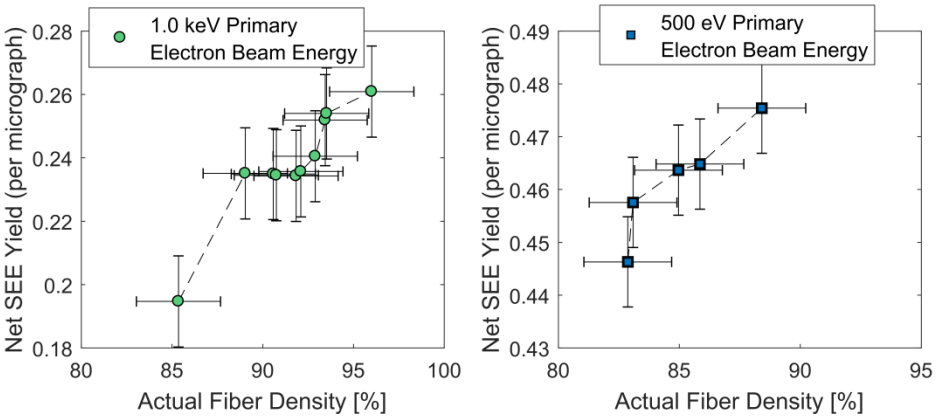

Figure 4. *The actual fiber density is plotted with total SEE yield several SEM micrographs of a carbon velvet sample that has 0.5mm fiber length and 85% indicated manufacturing packing density. (a) 1.0 keV primary electron beam energy and (b) 500 eV primary electron beam energy***.**

IV. Conclusions

Experimental measurements of carbon velvet samples with realistic and non-uniformly tilted fiber distributions show net SEE yields 29-65% lower than smooth graphite. There is also an indication of the existence of an optimal velvet configuration which for 1.5mm fiber length is between 68% and 81% actual fiber densities. This result is in agreement with theoretical models [3].

The technique of using SEM to quickly perform a qualitative SEE evaluation of a high aspect ratio velvet surface has been found to be useful for analyzing the velvet surface properties alongside its SEE yield. Results have also shown that the actual density of different regions of the same type of velvet sample is linearly related to the amount of SEE yield of such regions. This provides a quick approach to get an approximate measure of SEE yield without using complex laboratory setups (for example, in references [19] and [20]). A detailed analysis of these results will be reported in a separate journal paper.

Acknowledgments

The authors would like to thank Alex Merzhevskiy for technical assistance and Yao-Wen Yeh for many fruitful discussions regarding scanning electron microscopy. A.O, S. B and Y. R acknowledge support of this work by the US DOE and C. J acknowledges support of this fellowship at PPPL by the National Natural Science Foundation of China (No. 1150123, 11375126, 11435009), a project funded by China Postdoctoral Science Foundation.

References

[1] Y. Raitses, D. Staack, A. Dunaevsky and N. J. Fisch, *Operation of a segmented Hall thruster with low-sputtering carbon-velvet electrode*, J. Appl. Phys. 99, 036103 (2006).
[2] C. Swanson and I. D. Kaganovich, *Modeling of reduced effective secondary electron emission yield from a velvet surface*, J. Appl. Phys. 120, 213302 (2016)
[3] A. Dunavesky, Y. Raitses and N. J. Fisch, *Yield of Secondary Electron Emission from Ceramic Materials of Hall Thruster*, Phys. Plasmas, 10, 2574 (2003).\
[4] Y. Raitses, I. D. Kaganovich, A. Khrabrov, D. Sydorenko, N. J. Fisch, and A. Smolyakov, *Effect of Secondary Electron Emission on Electron Cross-Field Current in ExB Discharges*, IEEE Trans. Plasma Sci. 39, 995 (2011)
[5] S. Mazouffre, S. Tsikata, and J. Vaudolon, *Optimization of a wall-less Hall thruster*, J. Appl. Phys. 116, 243302 (2014).

[6] S. I. Krasheninnikov, A. Y. Pigarov, and W. Lee, *Physics of the edge plasma and first wall in fusion devices: synergistic effects* Plasma Phys. Control. Fusion 57, 044009 (2015).
[7] J. P. Gunn, *Evidence for strong secondary electron emission in the tokamak scrape-off layer* Plasma Phys. Control. Fusion 54, 085007 (2012).
[8] M. R. Baklanov, J. F. D. Marneffe, D. Shamiryan, A. M. Urbanowicz, H. Shi, and T. V. Rakhimova, *Fluorine atoms interaction with the nanoporous materials: experiment and DFT simulation* J. Appl. Phys. 113, 041101 (2013).
[9] R. Tschiersch, M. Bogaczyk, and H. E. Wagner, *Systematic investigation of the barrier discharge operation in helium, nitrogen, and mixtures: discharge development, formation and decay of surface charges* J. Phys. D: Appl. Phys. 47, 365204 (2014).
[10] D. Sydorenko, I. Kaganovich, Y. Raitses, and A. Smolyakov, *Breakdown of a Space Charge Limited Regime of a Sheath in a Weakly Collisional Plasma Bounded by Walls with Secondary Electron Emission* Phys. Rev. Lett. 103,
[11] Sydorenko D, Smolyakov A, Kaganovich I and Raitses *Kinetic simulation of secondary electron emission effects in Hall thrusters* Phys. Plasmas 13 014501 (2006)
[12] G. D. Hobbs, and J. A. Wesson, *Heat flow through a Langmuir sheath in the presence of electron emission* Plasma Physics 9, 85 (1967).
[13] M. T. F. Pivi, R. E. Kirby *Sharp Reduction of the Secondary Electron Emission Yield from Grooved Surfaces* Journal of Applied Physics Vol 104, (2008).
[14] M. Ye, Y. N. He, S. G. Hu, R. Wang *Suppression of secondary electron yield by microporous array structure* J. Applied Physics 113 074904, (2013).
[15] M. Ye, Y. N. *He Investigation into anomalous total secondary electron yield for micro-porous Ag surface under oblique incidence conditions* Journal of Applied Physics 114 (2013).
[16] M. Patino, Y. Raitses, and R. Wirz, *Secondary electron emission from plasma-generated nanostructured tungsten fuzz* Applied Physics Letter 109, 201602 (2016)
[17] Y. Raitses, I. D. *Kaganovich Electron Emission from Nano- and Micro- Engineered Materials Relevant to Electric Propulsion* 33 rd International Electric Propulsion Conference 390, (2013).
[18] C. Swanson, I. D. Kaganovich *"Feathered" fractal surfaces to minimize secondary electron emission for a wide range of incident angles* Journal of Applied Physics 122, 043301 (2017)
[19] C. Jin, A. Ottaviano, Y. Raitses, *Secondary electron emission yield from high aspect ratio carbon velvet surfaces,* Journal of Applied Physics (2017)
[20] M. I. Patino, Y. Raitses, B. E. Koel and R. E. Wirz *Analysis of secondary electron emission for conducting materials using 4-grid LEED/AES optics*, Journal of Physics D: Applied Physics 48, 195204 (2015)
[21] Goldstein, J., Newbury, D.E., Joy, D.C., Lyman, C.E., Echlin, P., Lifshin, E., Sawyer, L., Michael, J.R. *Scanning Electron Microscopy and X-ray Microanalyses*, New York : Kluwer Academic/Plenum Publishers (2003)